

Refined Bounds for Inter-Carrier Interference in OFDM due to Time-Varying Channels and Phase Noise

Tenneti Venkata Satya Sreedhar

Neelesh B. Mehta, *Fellow, IEEE*

Abstract—Inter-carrier interference (ICI) due to time-variations of the channel and phase noise is a critical issue in current orthogonal frequency division multiplexing (OFDM) systems. For the discrete-time formulation of OFDM and the general case of partially occupied contiguous subcarriers, we present exact expressions for the average ICI power at each subcarrier. These lead to insightful lower and upper bounds for the bandwidth-averaged ICI power, which bring out the combined impact of Doppler spread and phase noise statistics. The bounds are tighter than those in the literature, which employ a tractable, but less accurate, continuous-time formulation and assume infinitely many subcarriers.

Index Terms—phase noise, inter-carrier interference, OFDM, auto-correlation, Doppler spread, bounds.

I. INTRODUCTION

5G new radio (NR) based wireless systems use higher order modulation schemes and the large bandwidths available in mmWave frequency bands to meet the ever-increasing data rate requirements and boost network capacity. However, the higher carrier frequencies in the mmWave bands cause a large Doppler spread even in moderate mobility scenarios. Furthermore, instabilities in the local oscillators used for generating these carriers at the transmitter and receiver cause phase noise. Doppler spread and phase noise lead to inter-carrier interference (ICI) in an orthogonal frequency division multiplexing (OFDM) receiver, and can cause a severe degradation in its performance [1] [2]. Even in the sub-6 GHz bands, phase noise degrades the performance of the receiver for higher order modulation schemes.

To alleviate the effects of Doppler and phase noise, a numerology with a higher subcarrier spacing can be used to mitigate ICI at higher carrier frequencies. Additional demodulation reference signals can be transmitted to improve channel estimation in high-mobility scenarios. In addition, phase tracking reference signals (PTRSs) are transmitted to estimate and compensate the distortion caused by phase noise [3]. Therefore, a detailed analysis of the combined effects of Doppler and phase noise on OFDM in the context of 5G systems is essential.

T. V. S. Sreedhar is with the Central Research Laboratory at Bharat Electronics Limited, Bengaluru, India (email: sreedhartenneti@gmail.com).

Neelesh B. Mehta is with the Dept. of Electrical Communication Eng. at the Indian Institute of Science (IISc), Bengaluru, India (email: nbmehta@iisc.ac.in). This work was supported in part by the “Next Generation Wireless Research and Standardization on 5G and Beyond” project funded by Ministry of Electronics & Information Technology, Govt. of India.

A. Literature Survey

The literature on ICI and phase noise spans several decades. In [1], ICI in multiple-input-multiple-output (MIMO) OFDM systems is analyzed and time-domain mitigation techniques are proposed. In [4], channel estimation and detection methods are proposed for OFDM receivers impaired by ICI due to time-varying channels. In [5], insightful bounds are derived that bring out the quadratic dependence of the ICI power on Doppler spread. However, infinitely many subcarriers and a simpler continuous-time model are assumed. In the continuous-time model, the signal transmitted does not depend on the discrete Fourier transform (DFT) length; only the OFDM symbol duration matters [5]. In [6], bounds are derived again using a continuous-time formulation for the ICI power. While a more realistic discrete-time formulation is also considered, no bounds are derived from it.

In [7], measurements of error vector magnitude and phase error, after phase noise compensation, in a pre-5G mmWave testbed are compared with simulations. In [2], the mean square error of the transmitted data in mmWave time-varying channels impaired by phase noise is derived. In [8], a non-iterative solution using linear minimum mean squared-error estimation is proposed for the joint estimation problem of phase noise and channel in mmWave systems. To mitigate phase noise, a block PTRS structure is proposed for OFDM systems operating beyond 52.6 GHz in [9]. In [10], an analytical framework is proposed to specify the required power spectral density mask for phase noise in mmWave massive MIMO systems for a target signal-to-interference-noise ratio. In [11], an iterative, joint phase estimation and decoding algorithm is proposed for low density parity check and turbo codes in channels affected by phase noise.

B. Focus and Contributions

In this paper, we present an analysis of the ICI power encountered by OFDM systems that accounts for the combined effect of time-varying channels and phase noise.

- For the discrete-time model of the OFDM signal and channel, we derive exact expressions for the bandwidth-averaged ICI power in non-line-of-sight (NLoS) and line-of-sight (LoS) channels. The expressions account for the combined effect of time-variations in the channel and phase noise. They differ from the expressions in [5], which assume infinitely many subcarriers, use an analytically simpler – but less accurate – continuous-time

formulation, and do not consider phase noise. We find that the lower bound that this simplification leads to can even exceed the actual ICI. Our results also apply to the partially occupied case in which only some subcarriers are occupied and contiguous. This is unlike [5], [6], which assume that all the subcarriers are occupied.

- We then derive insightful bounds for the ICI power that bring out its dependence on Doppler spread, and phase noise bandwidth and variance. We observe that these bounds are tighter compared to those in [5] and [6] for the tapped delay line (TDL) LoS and NLoS channel models specified for 5G in 3GPP.

C. Outline and Notation

In Section II, we present the OFDM system model. In Section III, we analyze ICI in wideband fading channels in the presence of phase noise and derive bounds for its bandwidth-averaged power. Numerical results are presented in Section IV. Our conclusions follow in Section V.

Notation: The conjugate of a complex number z is denoted by z^* . The notation $X \sim \mathcal{CN}(\sigma^2)$ means that X is a zero-mean, circularly symmetric complex Gaussian random variable (RV) with variance σ^2 . Expectation is denoted by $\mathbb{E}[\cdot]$.

II. SYSTEM MODEL

Consider an OFDM system in which the transmitted signal is given by

$$s[n] = \sqrt{\frac{P_T}{Z}} \sum_{u=O}^{O+Z-1} \sum_{m=-\infty}^{\infty} x_{u,m} g[n - mN_T] \times e^{j\frac{2\pi u}{N}[n - N_{CP} - mN_T]}, \quad (1)$$

where $x_{u,m}$ is the symbol transmitted over subcarrier u of OFDM symbol m and N_T is the number of samples in the OFDM symbol duration including cyclic prefix. It has $Z \leq N$ contiguous occupied subcarriers with indices $O, O+1, \dots, O+Z-1$. The transmit power is P_T . Also, $\mathbb{E}[|x_{u,m}|^2] = 1$ and $N_T = N + N_{CP}$, where N is the DFT length. The OFDM symbol duration T_s equals NT_{samp} , where T_{samp} is the sampling duration, and the cyclic prefix duration T_{CP} equals $N_{CP}T_{\text{samp}}$. The transmit window $g[n]$ is 1 for $0 \leq n < N_T$, and is 0 otherwise.¹

The received signal $y[n]$ after passing through a wideband time-varying multipath channel is given by

$$y[n] = e^{j\phi[n]} \sum_{l=0}^{L-1} h_l[n] s[n-l] + \omega[n], \quad (2)$$

where $\{h_l[n]\}_{l=0}^{L-1}$ are the time-varying channel taps, which are zero-mean, wide sense stationary, and uncorrelated [12, Ch. 3], $\phi[n]$ is the phase noise at the receiver, and $\omega[n]$ is

¹In the continuous-time model, the continuous-time equivalent signal $s(t)$ of $s[n]$ is given by $s(t) = \sqrt{\frac{P_T}{Z}} \sum_{u=O}^{O+Z-1} \sum_{m=-\infty}^{\infty} x_{u,m} g(t - mT_s) e^{j\frac{2\pi u}{T_s}(t - T_{CP} - mT_s)}$. Note that this is not a function of N .

additive white Gaussian noise (AWGN) with variance σ^2 . The auto-correlation $r_l[w]$ of the l^{th} channel tap is

$$r_l[w] \triangleq \mathbb{E}[h_l[n+w] h_l^*[n]]. \quad (3)$$

For example, for the classical Jakes' fading model, we have $r_l[w] = r_l[0] J_0(2\pi f_d w T_{\text{samp}})$, where $J_0(\cdot)$ is the zeroth-order Bessel function of the first kind and f_d is the Doppler spread. Without loss of generality, let $\sum_{l=0}^{L-1} r_l[0] = 1$. The phase noise is a filtered wide-sense stationary Gaussian random process with bandwidth f_p and has a variance σ_ϕ^2 [13]. Its auto-correlation $r_\phi[w]$ is $r_\phi[w] \triangleq \mathbb{E}[\phi[n] \phi[n+w]]$.

The demodulated signal $\hat{y}_{k,m}$ at occupied subcarrier k of OFDM symbol m is given by

$$\hat{y}_{k,m} = \frac{1}{\sqrt{N}} \sum_{n=-\infty}^{\infty} y[n] q[n - mN_T] \times e^{-j\frac{2\pi k}{N}[n - N_{CP} - mN_T]}, \quad (4)$$

where $q[n]$ is the rectangular receive window; it is 1 for $N_{CP} \leq n < N_T$, and is 0 otherwise.

III. ICI ANALYSIS AND BOUNDS

From (4), the instantaneous ICI $I_{\text{ICI}}[k, m]$ at occupied subcarrier k , for $O \leq k \leq O+Z-1$, and OFDM symbol m can be shown to be

$$I_{\text{ICI}}[k, m] = \sqrt{\frac{P_T}{NZ}} \sum_{l=0}^{L-1} \sum_{u=O, u \neq k}^{O+Z-1} \sum_{n=N_{CP}+mN_T}^{(m+1)N_T-1} e^{j\phi[n]} h_l[n] \times x_{u,m} e^{j\frac{2\pi}{N}(u-k)[n - N_{CP} - mN_T]} e^{-j\frac{2\pi}{N}lu}. \quad (5)$$

The average ICI power at occupied subcarrier k is defined as $P_{\text{ICI}}[k] \triangleq \mathbb{E}[|I_{\text{ICI}}[k, m]|^2]$. It is not a function of m because the channel and phase noise are wide-sense stationary. The bandwidth-averaged ICI power \bar{P}_{ICI} is defined as

$$\bar{P}_{\text{ICI}} \triangleq \frac{1}{Z} \sum_{k=O}^{O+Z-1} P_{\text{ICI}}[k]. \quad (6)$$

Note that it averages $P_{\text{ICI}}[k]$ over the occupied subcarriers.

Result 1: The average ICI power $P_{\text{ICI}}[k]$ on occupied subcarrier k is given by

$$P_{\text{ICI}}[k] = \frac{P_T}{NZ} \sum_{u=O, u \neq k}^{O+Z-1} \sum_{w=-(N-1)}^{N-1} \sum_{l=0}^{L-1} e^{r_\phi[w] - \sigma_\phi^2} r_l[w] \times (N - |w|) e^{j\frac{2\pi}{N}(u-k)w}. \quad (7)$$

Proof: The proof is given in Appendix A. ■

We note that the average ICI power depends on the occupied subcarrier index k . This is unlike [6], in which the ICI power is the same for all subcarriers because the number of occupied subcarriers is equal to the DFT length. In such a case, every subcarrier has the same set of spectral distances to the remaining subcarriers. Substituting unity for the terms $r_\phi[w]$ and σ_ϕ^2 in (7) and simplifying yields the result in [1] for the single-input-single-output case and the expression in [4, (A7)].

As shown in Appendix B, the bandwidth-averaged ICI power is given by

$$\bar{P}_{\text{ICI}} = \frac{P_T}{NZ^2} \sum_{l=0}^{L-1} \sum_{w=-(N-1)}^{N-1} e^{r_\phi[w] - \sigma_\phi^2 r_l[w]} (N - |w|) \times \left[\left(\frac{\sin\left(\frac{\pi Z w}{N}\right)}{\sin\left(\frac{\pi w}{N}\right)} \right)^2 - Z \right]. \quad (8)$$

From (8), we see that \bar{P}_{ICI} depends on the total power P_T , the number of occupied subcarriers Z , the auto-correlation functions of the channel and the phase noise, and the DFT length N .² It is not a function of O .

The above result applies to LoS and NLoS fading channels. In an NLoS channel, $h_l[n] \sim \mathcal{CN}(r_l[0])$, for $0 \leq l \leq L-1$. In an LoS channel, the first tap $h_0[n]$ corresponds to a specular path. It can be written as $h_0[n] = \sqrt{r_0[0]} \left(\sqrt{\frac{K}{K+1}} e^{j\theta} + \sqrt{\frac{1}{K+1}} \tilde{h}_0[n] \right)$, where K is the Rician-factor, θ is a uniform RV over $[-\pi, \pi)$, and $\tilde{h}_0[n] \sim \mathcal{CN}(1)$. The auto-correlation for $h_0[n]$ then becomes $r_0[w] = r_0[0] \left(\frac{K + \tilde{r}_0[w]}{K+1} \right)$, where $\tilde{r}_0[w]$ is the auto-correlation of $\tilde{h}_0[n]$.

To gain more insights, consider the case without phase noise. Then, the expression for $P_{\text{ICI}}[k]$ in (7) simplifies to

$$P_{\text{ICI}}[k] = \frac{P_T}{NZ} \sum_{u=O, u \neq k}^{O+Z-1} \sum_{w=-(N-1)}^{N-1} \left[\hat{r}_0[w] + \sum_{l=1}^{L-1} r_l[w] \right] \times (N - |w|) e^{j \frac{2\pi}{N} (u-k)w}, \quad (9)$$

where $\hat{r}_0[w]$ is $\tilde{r}_0[w] r_0[0] / (K+1)$ and $r_0[w]$ for LoS and NLoS channels, respectively. For LoS channels, the specular component of the Rician tap does not contribute to the ICI power.

A. Bounds

Let $\bar{r}_l(\tau) \triangleq \mathbb{E} [e^{j(\phi(t+\tau) - \phi(t))} h_l(t+\tau) h_l^*(t)]$ denote the composite auto-correlation, which captures the combined effects of phase noise and Doppler spread. Let $\alpha_{1,l} = \int_{-\infty}^{\infty} f^2 S_l(f) df$ and $\alpha_{2,l} = \int_{-\infty}^{\infty} f^4 S_l(f) df$ denote the second and fourth moments, respectively, of the power spectrum $S_l(f)$ of $\bar{r}_l(\tau)$. Using the time-differentiation property of the Fourier transform, we can show that

$$\alpha_{1,l} = -\bar{r}_l''(0) / (4\pi^2) \quad \text{and} \quad \alpha_{2,l} = \bar{r}_l''''(0) / (16\pi^4), \quad (10)$$

where $\bar{r}_l''(\tau)$ and $\bar{r}_l''''(\tau)$ are the second and fourth derivatives, respectively, of $\bar{r}_l(\tau)$. In terms of the individual auto-

²For the general case of non-contiguous subcarriers, when the indices of the occupied subcarriers are k_0, k_1, \dots, k_{Z-1} , \bar{P}_{ICI} can be shown to be

$$\bar{P}_{\text{ICI}} = \frac{P_T}{NZ^2} \sum_{i=0}^{Z-1} \sum_{j=0, j \neq i}^{Z-1} \sum_{w=-(N-1)}^{N-1} \sum_{l=0}^{L-1} e^{r_\phi[w] - \sigma_\phi^2 r_l[w]} (N - |w|) \times e^{j \frac{2\pi}{N} (k_j - k_i)w}.$$

correlations for phase noise and channel, we can show that

$$\alpha_{1,l} = -\left(r_l''(0) + 2r_l'(0)r_\phi'(0) + r_l(0) \left[r_\phi''(0) + (r_\phi'(0))^2 \right] \right) / (4\pi^2), \quad (11)$$

$$\alpha_{2,l} = \left(r_l''''(0) + 4r_l'''(0)r_\phi'(0) + 6r_l''(0) \left[r_\phi''(0) + (r_\phi'(0))^2 \right] + 4r_l'(0) \left[r_\phi'''(0) + 3r_\phi'(0)r_\phi''(0) + (r_\phi'(0))^3 \right] + r_l(0) \left[r_\phi''''(0) + 3(r_\phi''(0))^2 + 6(r_\phi'(0))^2 r_\phi''(0) + (r_\phi'(0))^4 + 4r_\phi'''(0)r_\phi'(0) \right] \right) / (16\pi^4). \quad (12)$$

Result 2: In an NLoS channel, the bandwidth-averaged ICI power \bar{P}_{ICI} is lower and upper bounded as follows:

$$\bar{P}_{\text{ICI}} \leq \frac{P_T}{NZ^2} \left[NZ(Z-N) + 2\psi[0, Z] + \frac{\alpha_2}{12} \psi[4, Z] \left(\frac{2\pi T_s}{N} \right)^4 + \frac{\alpha_1}{12} [ZN^2(N^2-1) - 12\psi[2, Z]] \left(\frac{2\pi T_s}{N} \right)^2 \right], \quad (13)$$

$$\bar{P}_{\text{ICI}} \geq \frac{P_T}{NZ^2} \left[NZ(Z-N) + 2\psi[0, Z] - \frac{\alpha_2}{12} Z\psi[4, 1] \left(\frac{2\pi T_s}{N} \right)^4 + \frac{\alpha_1}{12} [ZN^2(N^2-1) - 12\psi[2, Z]] \left(\frac{2\pi T_s}{N} \right)^2 \right], \quad (14)$$

where $\alpha_1 = \sum_{l=0}^{L-1} \alpha_{1,l}$, $\alpha_2 = \sum_{l=0}^{L-1} \alpha_{2,l}$, and the function ψ is defined as

$$\psi[p, q] \triangleq \sum_{w=1}^{N-1} w^p (N-w) \left(\frac{\sin(\pi w q / N)}{\sin(\pi w / N)} \right)^2. \quad (15)$$

Proof: The proof is given in Appendix C. ■

The coefficients α_1 and α_2 capture the combined effect of Doppler spread and phase noise. For example, when the phase noise has a uniform power spectrum (which lies between $-f_p$ and f_p) and the channel taps follow the Jakes' Doppler spectrum, $\alpha_1 = f_d^2/2 + f_p^2 \sigma_\phi^2/3$ and $\alpha_2 = 3f_d^4/8 + f_d^2 f_p^2 \sigma_\phi^2/2 + f_p^4 (\sigma_\phi^2/5 + \sigma_\phi^4/3)$. Thus, the ICI power is proportional to the sum of the squares of the Doppler spread and the phase noise variance multiplied by the square of the phase noise bandwidth. The above bounds show that the ICI power depends upon the DFT length N and the number of occupied subcarriers Z . The bounds for the LoS channel case can be obtained similarly and are not shown to conserve space.

IV. NUMERICAL RESULTS

We now present Monte Carlo simulation results to understand the behavior of the ICI power and evaluate the tightness of its bounds for the partially occupied subcarriers

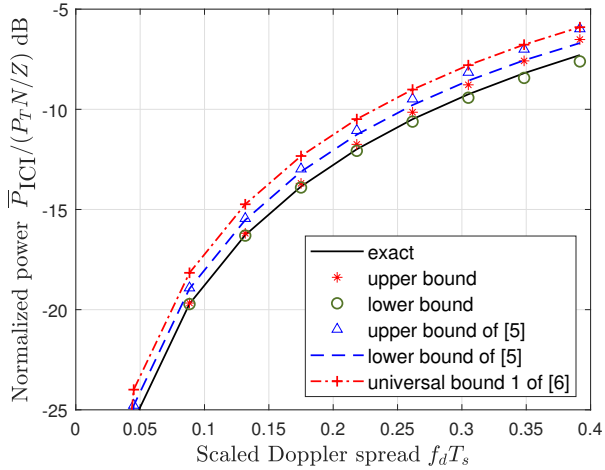


Fig. 1. Normalized bandwidth-averaged ICI power and bounds in TDL-C NLoS channel ($N = 64$, $Z = 16$, $T_s = 66.67 \mu\text{s}$, and a delay spread of 100 ns).

case for different values of Z and N . The subcarrier spacing is 15 kHz, the sampling rate is 7.68 MHz, and the OFDM symbol duration is $66.67 \mu\text{s}$. We use the TDL-C and TDL-D channel models that are specified in 5G NR for NLoS and LoS channels, respectively [14, Tables 7.7.2-3, 7.7.2-4]. Each tap undergoes Jakes' fading. The TDL-C model has 24 taps. The TDL-D model has 13 taps and a larger delay spread. Its first LoS tap has a Rician-factor of 13.3 dB. The phase noise has a uniform power spectral density between $-f_p$ and f_p Hz. The simulation results are averaged over 10000 channel and phase noise realizations. The ICI powers and bounds are normalized with respect to the power per subcarrier.

Fig. 1 plots the normalized bandwidth-averaged ICI power and its lower and upper bounds as a function of the scaled Doppler spread $f_d T_s$ for the TDL-C channel model with a delay spread of 100 ns. We benchmark our results with the upper and lower bounds from [5], and the universal bound 1 from [6], all of which are based on a continuous-time formulation and assume that N is large and $Z = N$. Since the bounds in [5] and [6] apply without phase noise, we do not consider phase noise in this plot. We observe that our upper and lower bounds are both tight. The lower bound is indistinguishable from the exact curve even at large values of $f_d T_s$. On the other hand, the lower bound in [5, (3.9)] can even exceed the exact value for smaller N due to the simplifications made by the continuous-time formulation. The upper bound is tighter than the upper bound of [5, (3.10)] and the universal bound 1 of [6, (25)] by 0.6 to 0.8 dB and 0.6 to 1.6 dB, respectively.

Fig. 2 plots the normalized bandwidth-averaged ICI power as a function of the scaled phase noise bandwidth $f_p T_s$ for different Doppler spreads and different numbers of occupied subcarriers for the TDL-D channel model with a delay spread of 100 ns. f_p ranges from 10 Hz to 3.7 kHz. Also shown are the normalized bounds and the normalized ICI power at

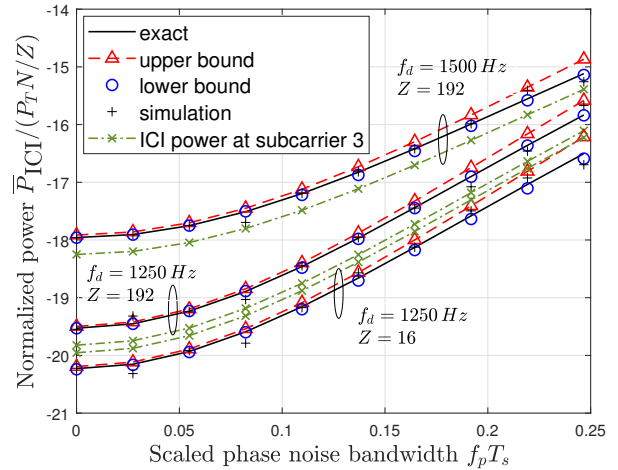


Fig. 2. Normalized bandwidth-averaged ICI power in TDL-D LoS channel ($N = 256$, delay spread of 100 ns, $\sigma_\phi = 0.5$ radians, and $T_s = 66.67 \mu\text{s}$).

subcarrier 3. We see that both bounds are tight. The ICI power at subcarrier 3 is not equal to the bandwidth-averaged ICI power because not all subcarriers are occupied. This is in contrast to the $Z = N$ case considered in [6], where every subcarrier has the same ICI power. As Z/N increases, the normalized ICI power increases.

V. CONCLUSIONS

We derived expressions for the average ICI power in LoS and NLoS channels, which captured the combined effect of the Doppler spread and phase noise. Our approach employed the more realistic discrete-time model. It applied to the case in which only fraction of subcarriers were occupied and were contiguous. This led to the ICI power being different for different subcarriers. We also derived insightful lower and upper bounds for the bandwidth-averaged ICI power. They brought out its dependence on the Doppler spread, phase noise variance, number of occupied subcarriers, and phase noise bandwidth. Both bounds were tight over a wide range of Doppler spreads and phase noise bandwidths. They were much tighter than the ones in the literature, which employed a simpler, but less accurate, continuous-time formulation and assumed an infinite number of subcarriers.

APPENDIX

A. Proof of Result 1

Let $\bar{h}_l[n] = e^{j\phi[n]} h_l[n]$; we shall refer to it as the composite channel's l^{th} tap. Since $\{h_l[n]\}_{l=0}^{L-1}$ are uncorrelated and are independent of $\phi[n]$, $\{\bar{h}_l[n]\}_{l=0}^{L-1}$ are also uncorrelated. The auto-correlation $\bar{r}_l[w]$ of the composite channel taps is given by

$$\bar{r}_l[w] = \mathbb{E} \left[\bar{h}_l[n+w] \bar{h}_l^*[n] \right]. \quad (16)$$

The transmit symbols $\{x_{u,m}\}_{u=0}^{O+Z-1}$ are independent and identically distributed with zero-mean and unit variance.

Therefore, substituting $n' = n - N_{CP} - mN_T$ in (5) and simplifying, we get

$$P_{CI}[k] = \frac{P_T}{NZ} \sum_{u=O, u \neq k}^{O+Z-1} \sum_{l=0}^{L-1} \mathbb{E} \left[\left| \sum_{n'=0}^{N-1} \bar{h}_l[n' + N_{CP} + mN_T] \times e^{j\frac{2\pi}{N}(u-k)n'} \right|^2 \right]. \quad (17)$$

Expanding the expectation terms using (16), and applying the transformation $s - t = w$, we get

$$P_{CI}[k] = \frac{P_T}{NZ} \sum_{u=O, u \neq k}^{O+Z-1} \sum_{l=0}^{L-1} \sum_{w=-(N-1)}^{N-1} \bar{r}_l[w] (N - |w|) \times e^{j\frac{2\pi}{N}(u-k)w}. \quad (18)$$

As the phase noise is independent of the channel tap gains, we get

$$\bar{r}_l[w] = \mathbb{E} \left[e^{j(\phi[n+w] - \phi[n])} \right] r_l[w]. \quad (19)$$

Since $\phi[n]$ is a wide-sense stationary Gaussian random process, $(\phi[n+w] - \phi[n])$ is a zero-mean Gaussian RV with variance $2\sigma_\phi^2 - 2r_\phi[w]$. Its moment generating function $\mathbb{E} [e^{t(\phi[n+w] - \phi[n])}]$ evaluated at $t = j$ is $e^{r_\phi[w] - \sigma_\phi^2}$. Substituting this in (19), we get

$$\bar{r}_l[w] = e^{r_\phi[w] - \sigma_\phi^2} r_l[w]. \quad (20)$$

Substituting (20) in (18) yields (7).

B. Derivation of (8)

Substituting (7) in (6), $k' = k - O, u' = u - O$, and changing the order of summation, we get

$$\bar{P}_{ICI} = \frac{P_T}{NZ^2} \sum_{l=0}^{L-1} \sum_{w=-(N-1)}^{N-1} e^{r_\phi[w] - \sigma_\phi^2} r_l[w] (N - |w|) \sum_{k'=0}^{Z-1} e^{-j\frac{2\pi}{N}k'w} \sum_{u'=0, u' \neq k'}^{Z-1} e^{j\frac{2\pi}{N}u'w}. \quad (21)$$

Now, $\sum_{u'=0, u' \neq k'}^{Z-1} e^{j\frac{2\pi}{N}u'w} = \frac{\sin(\frac{\pi Z w}{N})}{\sin(\frac{\pi w}{N})} e^{j\frac{2\pi}{N}(Z-1)w} - e^{j\frac{2\pi}{N}k'w}$

and $\sum_{k'=0}^{Z-1} e^{-j\frac{2\pi}{N}k'w} \sum_{u'=0, u' \neq k'}^{Z-1} e^{j\frac{2\pi}{N}u'w} = \frac{\sin^2(\frac{\pi Z w}{N})}{\sin^2(\frac{\pi w}{N})} - Z$. Substituting these in (21) yields (8).

C. Proof of Result 2

We start directly from the upper and lower bounds that are derived in [5, Sec. III-B] for the auto-correlation $\bar{r}_l[w]$ of the l^{th} composite channel tap. These use the inequality $(\theta^2/2) - (\theta^4/24) \leq 1 - \cos \theta \leq (\theta^2/2)$. We obtain the following two inequalities for $\bar{r}_l[w]$:

$$\bar{r}_l[w] \geq \bar{r}_l[0] - \frac{\alpha_{1,l}}{2} \left(\frac{2\pi f_d w T_s}{N} \right)^2, \quad (22)$$

$$\bar{r}_l[w] \leq \bar{r}_l[0] - \frac{\alpha_{1,l}}{2} \left(\frac{2\pi f_d w T_s}{N} \right)^2 + \frac{\alpha_{2,l}}{24} \left(\frac{2\pi f_d w T_s}{N} \right)^4. \quad (23)$$

Substituting the upper bound (23) for $\bar{r}_l[w]$ and lower bound (22) for $-\bar{r}_l[w]$ in (8), we get

$$\begin{aligned} \bar{P}_{ICI} &\leq \frac{P_T}{NZ^2} \sum_{l=0}^{L-1} \left[\bar{r}_l[0] NZ (Z-1) \right. \\ &\quad \left. + 2Z \sum_{w=1}^{N-1} \left(\frac{\alpha_{1,l}}{2} \left(\frac{2\pi w T_s}{N} \right)^2 - \bar{r}_l[0] \right) (N-w) \right. \\ &\quad \left. + 2 \sum_{w=1}^{N-1} \left(\bar{r}_l[0] - \frac{\alpha_{1,l}}{2} \left(\frac{2\pi w T_s}{N} \right)^2 + \frac{\alpha_{2,l}}{24} \left(\frac{2\pi w T_s}{N} \right)^4 \right) \right. \\ &\quad \left. \times (N-w) \left(\frac{\sin(\frac{\pi Z w}{N})}{\sin(\frac{\pi w}{N})} \right)^2 \right]. \quad (24) \end{aligned}$$

Substituting $\sum_{w=1}^{N-1} w^2 (N-w) = N^2 (N^2 - 1) / 12$ and $\sum_{l=0}^{L-1} \bar{r}_l[0] = 1$, using the definition of the function ψ in (15), and rearranging terms, we get (13). Substituting the lower bound in (22) for $\bar{r}_l[w]$ and upper bound in (23) for $-\bar{r}_l[w]$ in (8), and simplifying along the above lines yields (14).

REFERENCES

- [1] A. Stamoulis, S. N. Diggavi, and N. Al-Dhahir, "Intercarrier interference in MIMO OFDM," *IEEE Trans. Signal Process.*, vol. 50, no. 10, pp. 2451–2464, Oct. 2002.
- [2] H. Iimori, G. T. F. deAbreu, D. G. González, and O. Gonsa, "Mitigating channel aging and phase noise in millimeter wave MIMO systems," *IEEE Trans. Veh. Technol.*, vol. 70, no. 7, pp. 7237–7242, Jul. 2021.
- [3] Y. Qi, M. Hunukumbure, H. Nam, H. Yoo, and S. Amuru, "On the phase tracking reference signal (PT-RS) design for 5G new radio (NR)," in *Proc. VTC (Fall)*, Apr. 2019, pp. 1–5.
- [4] Y. S. Choi, P. J. Voltz, and F. A. Cassara, "On channel estimation and detection for multicarrier signals in fast and selective Rayleigh fading channels," *IEEE Trans. Commun.*, vol. 49, no. 8, pp. 1375–1387, Aug. 2001.
- [5] Y. Li and L. J. Cimini, "Bounds on the interchannel interference of OFDM in time-varying impairments," *IEEE Trans. Commun.*, vol. 49, no. 3, pp. 401–404, Mar. 2001.
- [6] X. Cai and G. B. Giannakis, "Bounding performance and suppressing intercarrier interference in wireless mobile OFDM," *IEEE Trans. Commun.*, vol. 51, no. 12, pp. 2047–2056, Dec. 2003.
- [7] J. Oh and T. K. Kim, "Phase noise effect on millimeter-wave pre-5G systems," *IEEE Access*, vol. 8, pp. 187 902–187 913, Oct. 2020.
- [8] M. Chung, L. Liu, and O. Edfors, "Phase-noise compensation for OFDM systems exploiting coherence bandwidth: Modeling, algorithms, and analysis," *IEEE Trans. Wireless Commun.*, vol. 21, no. 5, pp. 3040–3056, 2022.
- [9] T. Levanen, O. Tervo, K. Pajukoski, M. Renfors, and M. Valkama, "Mobile communications beyond 52.6 GHz: Waveforms, numerology, and phase noise challenge," *IEEE Wireless Commun. Mag.*, vol. 28, no. 1, pp. 128–135, Feb. 2021.
- [10] M. E. Rasekh, M. Abdelghany, U. Madhow, and M. Rodwell, "Phase noise in modular millimeter wave massive MIMO," *IEEE Trans. Wireless Commun.*, vol. 20, no. 10, pp. 6522–6535, Oct. 2021.
- [11] A. Kreimer and D. Raphaeli, "Efficient low-complexity phase noise resistant iterative joint phase estimation and decoding algorithm," *IEEE Trans. Commun.*, vol. 66, no. 9, pp. 4199–4210, Sep. 2018.
- [12] A. J. Goldsmith, *Wireless Communications*, 2nd ed. Cambridge Univ. Press, 2005.
- [13] F. Munier, T. Eriksson, and A. Svensson, "An ICI reduction scheme for OFDM system with phase noise over fading channels," *IEEE Trans. Commun.*, vol. 56, no. 7, pp. 1119–1126, Jul. 2008.
- [14] "Study on channel model for frequency spectrum above 6 GHz (release 15)," 3rd Generation Partnership Project (3GPP), Tech. Rep. 38.900 (v15.0.0), 2017.